Journal of Pharmaceutical and Biomedical Analysis 53 (2010) 843–851

Contents lists available at ScienceDirect

Journal of Pharmaceutical and Biomedical Analysis

journal homepage: www.elsevier.com/locate/jpba

Development of nitrosyl ruthenium complex-loaded lipid carriers for topical administration: improvement in skin stability and in nitric oxide release by visible light irradiation

Franciane Marquele-Oliveira[a], Danielle Cristine de Almeida Santana[a], Stephânia Fleury Taveira[a], Deise Mirella Vermeulen[a], Anderson Rodrigo Moraes de Oliveira[b], Roberto Santana da Silva[c], Renata Fonseca Vianna Lopez[a,*]

[a] Department of Pharmaceutical Sciences, School of Pharmaceutical Sciences of Ribeirão Preto, University of São Paulo, Av. do Café s/n, 14040-903, Ribeirão Preto, SP, Brazil
[b] Departamento de Química, Faculdade de Filosofia, Ciências e Letras de Ribeirão Preto, Universidade de São Paulo, 14040-901, Ribeirão Preto, SP, Brazil
[c] Department of Physics and Chemistry, School of Pharmaceutical Sciences of Ribeirão Preto, University of São Paulo, Ribeirão Preto, SP, Brazil

ARTICLE INFO

Article history:
Received 1 February 2010
Received in revised form 20 April 2010
Accepted 14 June 2010
Available online 19 June 2010

Keywords:
Nitrosyl ruthenium complexes
NO photorelease
Solid lipid nanoparticles
Nanostructured lipid carriers

ABSTRACT

The prominent nitric oxide (NO) donor [Ru(terpy)(bdqi)NO](PF$_6$)$_3$ has been synthesized and evaluated with respect to noteworthy biological effects due to its NO photorelease, including vascular relaxation and melanoma cell culture toxicity. The potential for delivering NO in therapeutic quantities is tenable since the nitrosyl ruthenium complex (NRC) must first reach the "target tissue" and then release the NO upon stimulus. In this context, NRC-loaded lipid carriers were developed and characterized to further explore its topical administration for applications such as skin cancer treatment. NRC-loaded solid lipid nanoparticles (SLN) and nanostructured lipid carriers were prepared via the microemulsification method, with average diameters of 275 ± 15 nm and 211 ± 31 nm and zeta potentials of −40.7 ± 10.4 mV and −50.0 ± 7.5 mV, respectively. *In vitro* kinetic studies of NRC release from nanoparticles showed sustained release of NRC from the lipid carriers and illustrated the influence of the release medium and the lyophilization process. Stability studies showed that NO is released from NRC as a function of temperature and time and due to skin contact. The encapsulation of NRC in SLN followed by its lyophilization, significantly improved the complex stability. Furthermore, of particular interest was the fact that in the NO photorelease study, the NO release from the NRC-loaded SLN was approximately twice that of just NRC in solution. NRC-loaded SLN performs well enough at releasing and protecting NO degradation *in vitro* that it is a promising carrier for topical delivery of NO.

1. Introduction

For at least three decades, nitric oxide (NO) has been known as an important signaling molecule in a wide variety of physiological processes, such as blood pressure regulation, inhibition of smooth muscle proliferation, platelet aggregation, immune response, and cell death [1,2]. In recent years, various exogenous NO donors have been synthesized to modulate NO concentrations in cellular environments in order to control the physiological processes it regulates. To date, the use of exogenous NO donors has been explored to treat hypertension and episodes of angina pectoris [3,4], as well as to kill malignant cells [5]. Indeed, NO has been shown to induce both apoptosis (programmed cell death) and cell destruction at elevated concentrations (mM range) [6].

Transition metal complexes of NO (metal nitrosyls) are one such class of NO donors. Since complexes of ruthenium are generally more stable, a variety of nitrosyl ruthenium complexes (NRC) have been isolated and studied in detail in terms of their NO donating capacities [2]. Those based in ruthenium (II) have received special attention. Coordination compounds containing the {Ru–NO} bond have been successfully employed as NO delivery agents, either by accessing the reduction potential of nitrosyl ligand [7–9] or by light stimulation [10–14].

The [Ru(terpy)(bdqi)NO](PF$_6$)$_3$ (bdqi = 1,2 benzoquinonediimine; terpy = terpyridine) complexes [15,16] (Fig. 1) have been explored extensively in an attempt to assess their therapeutic application due to the NO release. Employing this NRC has resulted in significant vascular relaxation due to the NO release from the complex [15,17,18]. Experiments currently being carried out have also demonstrated that this complex presents high toxicity in melanoma cell cultures under light stimulus, as it has been reported in literature for other exogenous NO donors [6,19]. Additionally,

* Corresponding author. Tel.: +55 16 36 02 42 02; fax: +55 16 36 02 42 02.
E-mail address: rvianna@fcfrp.usp.br (R.F.V. Lopez).

0731-7085/$ – see front matter © 2010 Elsevier B.V. All rights reserved.
doi:10.1016/j.jpba.2010.06.007

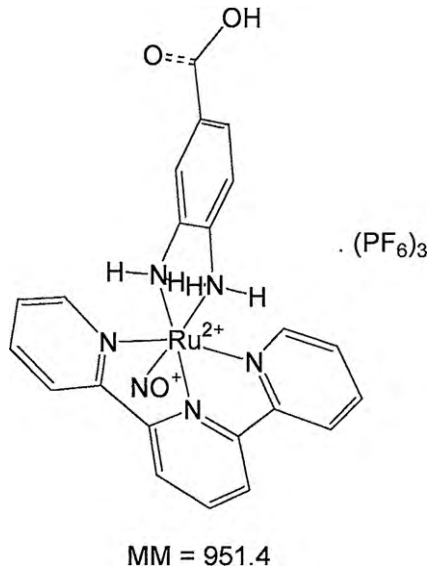

Fig. 1. Structure of the nitrosyl ruthenium complex.

the microsomal metabolism of this ruthenium complex was elucidated together with the demonstration of the isomerization of this NRC during its synthesis and the validation of an HPLC method for its determination in biological medium [20,21]. These publications [20,21] have served as base to the development and validation of the HPLC method employed in the present work for NRC determination in the lipid carriers and in skin samples once our objective is the administration of this new NRC in therapeutics, especially against skin cancer.

It is well established that the controlled (favorably triggered) release of NO at a selected site is critical for the successful employment of an NO donor in treating tumors and localized malignancies such as skin cancer. Thus, the NRC must first reach the "target tissue" and then release the NO upon stimulus, since the NO is a diffusible gas with a half-life of merely seconds [22] that could easily dissipate to the environment.

In general, drug topical administration is a challenge in pharmaceutics [23]. Some concerns must be considered regarding the topical application of NRC because it has a high molecular weight (951.4) and a positive electric charge, neither of which is favorable for penetrating skin. Moreover, it has been reported that the superficial lipophilic layer of the skin, the stratum corneum (SC), is a major barrier to the cutaneous delivery of hydrophilic molecules [24], such as the [Ru(terpy)(bdqi)NO]$(PF_6)_3$ complex. Therefore, a suitable release system is required to enable its successful therapeutic application. Lipid nanoparticles, due to the safety of the component materials, high physical stability, low cost, and controlled release abilities, show great potential and have generated great interest in the industrial and academic arenas [25,26]. Additionally, lipid nanoparticles may improve epidermal penetration because lipid carriers attach themselves to the skin surface, allowing lipid exchange between the outermost layers of the SC and the carrier [23].

The first generation of lipid nanoparticles was introduced as solid lipid nanoparticles (SLN) in the early 1990s; these were produced from solid lipids only. In the second generation technology of nanostructured lipid carriers (NLC), the particles began to be produced using a blend of solid and liquid lipids with the intention of increased drug loading [26].

Many different drugs have been incorporated in SLN and NLC. For example, epidermal targeting drugs include coenzyme Q10 [27], tretinoin [28], glucocorticoids [29,30], and cancer chemotherapy drugs, including doxorubicin [31] and methotrexate [32], among others.

In view of this, exploring the potential of SLN and NLC for improving the topical delivery of [Ru(terpy)(bdqi)NO]$(PF_6)_3$ is worthwhile. The long-term goal of this work is to develop topical NRC-carriers with an epidermal targeting effect for the treatment of skin cancer. The present study focused on the development, characterization, and assessment of potential for controlled release of NRC-lipid carriers. The NO release from NRC-loaded lipid carriers due to visible light irradiation was also assessed.

2. Material and methods

2.1. Materials

[Ru(terpy)(bdqi)NO]$(PF_6)_3$ (bdqi = 1,2 benzoquinonediimine; terpy = terpyridine) complex was synthesized as previously described [15] with minor modifications. Its purity was assessed by high-performance liquid chromatography (HPLC) and infrared spectroscopy (IR). Ruthenium chloride (III), bdqi (1,2 benzoquinonediimine) and 2,2′:6′,2″-terpiridine were obtained from Aldrich Chemicals (Saint Louis, MO, USA). Hepes (4-(2-hydroxyethyl)-1-piperazineethanesulfonic acid) was obtained from J.T. BAKER (Phillipsburg, USA). Lecithin (soybean lecithin at 99% of phosphatidylcholine) was supplied by Lipoid (Ludwigshafen, Germany). Stearic acid (95%) was supplied by Vetec (São Paulo, Brasil). Taurodeoxycholate acid sodium (97%) was supplied from Sigma–Aldrich (Deisenhofen, Germany). Oleic acid (99%) was obtained from Fluka (Buchs, Switzerland). Chromatographic-grade methanol was purchased from Merck (Darmstadt, Germany). Trifluoroacetic acid (TFA) was supplied by Tedia (Fairfield, USA). All other reagents were of analytical grade. The purified water used to prepare lipid carriers or mobile phase was purified in a Milli-Q-plus System (Millipore, Bedford, MA, USA).

2.2. Skin

Pig-ears were collected immediately after the slaughter of the animals (Frigorífico Pontal Ltda, Brazil). Ears were then kept at 4 °C while transported to the laboratory to be dermatomed. This whole process took no more than 2 h. After that, the dermatomed skin (700 μm) was kept at −20 °C and used for a maximum of 30 days.

2.3. Identification of [Ru(terpy)(bdqi)NO]$(PF_6)_3$ by HPLC

The identification of [Ru(terpy)(bdqi)NO]$(PF_6)_3$ by HPLC was performed as described by de Oliveira et al. [21] with minor modifications. Analyses were conducted using a Shimadzu LC10-AD (Kyoto, Japan) liquid chromatograph equipped with an LC10-AT solvent pump, a SIL-10AD automatic injector, and a SPD-A detector operating at 290 nm. Data were collected using CLASS-VP software. The separation of [Ru(terpy)(bdqi)NO]$(PF_6)_3$ was carried out at 37 (±2) °C on a LiChrospher RP – 18 (5 μm, 250 mm × 4 mm) – Merck, (Darmstadt, Germany) using an aqueous solution of trifluoroacetic acid 1% phosphate buffer pH 7:methanol (85:15, v/v) as a mobile phase at a flow rate of 1 mL min^{-1}. A CN guard column (4 mm × 4 mm, 5-μm particle size, Merck, Darmstadt, Germany) was used. Analytical curves of [Ru(terpy)(bdqi)NO]$(PF_6)_3$ solutions were prepared daily in Hepes buffer (25 mmol L^{-1}, containing NaCl 133 mmol L^{-1}, pH 7.4) and in purified water in the concentration range of 0.2-20 μg mL^{-1} and were protected from direct light.

2.3.1. Validation of the method

The method was validated following FDA recommendations [33]. Calibration curves were obtained by spiking aliquots of 5 mL Hepes buffer (25 mmol L^{-1}, containing NaCl 133 mmol L^{-1},

pH 7.4) with standard solutions of [Ru(terpy)(bdqi)NO](PF$_6$)$_3$ in the concentration range of 0.2–20 μg mL^{-1}. The sensitivity of the method was evaluated by determining the quantification limit (LOQ). The LOQ was defined as the lowest concentration that could be determined with accuracy and precision below 20% [33] over five analytical run and it was assessed at the concentration of 0.2 μg mL^{-1} of [Ru(terpy)(bdqi)NO](PF$_6$)$_3$. Precision was expressed as relative standard deviation (RSD %) and accuracy as percent of deviation between the true and the measured value (relative error, *E*%). To assess within-day precision and accuracy, replicate analyses (n = 5) of 5 mL Hepes buffer (25 mmol L^{-1}, containing NaCl 133 mmol L^{-1}, pH 7.4) spiked with concentrations of 2, 5 and 10 μg mL^{-1} of [Ru(terpy)(bdqi)NO](PF$_6$)$_3$ were performed. For between-day assays, solutions of [Ru(terpy)(bdqi)NO](PF$_6$)$_3$ (n = 5) were analyzed for three alternated days. The selectivity of the method was assured by analyzing blank lipid carriers, blank receiver solutions, as well as, blank skin homogenates. The recovery of [Ru(terpy)(bdqi)NO](PF$_6$)$_3$ extracted from the skin samples spiked with the NRC was determined using calibration curves obtained from the data of the analyte submitted to extraction using water as "sample" matrix at the same final volume (3 mL). The recovery was expressed as percentage of the amount extracted.

2.4. Lipid carrier preparation and characterization

SLN and NLC were obtained by the microemulsion method as described previously [32] with minor modifications. SLNs were prepared using stearic acid as the internal phase, soya lecithin as surfactant, sodium taurodeoxycholate as co-surfactant, and purified water as the continuous phase. Several lipid:surfactant:co-surfactant:water ratios were employed to obtain the microemulsion. Finally, the microemulsion for the SLN was prepared as follows: stearic acid (20%) was first melted 10 °C above its melting point (65.0–70.0 °C), then surfactant (10%) and NRC (0.8%) were added and stirred until completely solubilized. The aqueous phase (sufficient to prepare 1 g of microemulsion) together with the co-surfactant (2.5%) was heated to 80 °C and added to the melted lipid mixture. The mixture was maintained stirring at 80 °C until the microemulsion was formed. The resulting warm microemulsion was then dispersed into purified water at 2–5 °C under mechanical stirring (12,000 rpm) for 10 min (Ultra Turrax, AT15, IKA-Werke, Germany). NLC were obtained by replacing 50 mg of the stearic acid with oleic acid. SLN and NLC formulations containing no nitrosyl complex were also prepared. In some cases, as forwarded described, the SLN were lyophilized employing sucrose, as cryoprotector (8%). The lyophilized SLN were readily resuspended in water when necessary.

2.4.1. Photon correlation spectroscopy

The average diameter and polydispersity index (PdI) of SLN and NLC were measured by photon correlation spectroscopy (PCS) (Malvern Zetasizer Nano ZS90, Malvern instruments Ltd., UK) with a 50 mV laser. Typically, 0.02 mL of SLN or NLC was diluted by 2 mL of purified water before adding into the sample cell. The measurements were performed at 25.0 °C at a fixed angle of 173.0°. The measurement time was 60 s. Each value reported is the average of at least three measurements. The polydispersity index can reflect the size distribution of particle population.

2.4.2. Determination of zeta potential

The zeta potential of the lipid carriers was measured by Malvern Zetasizer Nano ZS90 (Malvern instruments Ltd., UK). Prior to the measurements, the SLN and NLC samples were diluted with 1:10 in NaCl (10%). Each sample was analyzed in triplicate.

2.4.3. Scanning electron microscopy (SEM)

The morphology of SLN and NLC was viewed using a field emission gun scanning electron microscopy (FEG-SEM) (FEG XL30, Phillips) at an accelerating voltage of 20 kV. One drop of the nanoparticle suspension was placed on a graphite surface. After drying at room temperature, the sample was coated with gold using ion sputtering.

2.4.4. Entrapment efficiency

The entrapment efficiency (EE), which corresponds to the percentage of NRC encapsulated within and adsorbed on the nanoparticles, was determined by the difference between the concentration of free particles and the total concentration of the nitrosyl complex in the dispersion medium [34,28]. Thus, 1 mL of SLN or NLC dispersion was transferred to the upper chamber of AMICON ultra centrifuge tubes fitted with an ultrafilter (NWCO100KD) (Millipore, Bedford, USA). The tubes were centrifuged at 3200 × g (Eppendorf centrifuge, 5810R, Hamburg, Germany) for 20 min. The filtrate was analyzed for unencapsulated NRC by the HPLC method described above.The entrapment efficiency was calculated by the following equation:

$$\mathrm{EE\%} = \left[\frac{M_{\text{total drug}} - M_{\text{free drug}}}{M_{\text{total drug}}}\right] 100$$

where $M_{\text{total drug}}$ is the mass of total drug in the whole aqueous dispersion and the $M_{\text{free drug}}$ is the mass of free drug detected in the filtrate of the aqueous dispersion.

Total drug in the aqueous dispersion was obtained by solubilizing an aliquot of the SLN or NLC dispersion in methanol, then diluting it with purified water, filtering, and injecting it into the HPLC apparatus.

2.5. In vitro kinetics of [Ru(terpy)(bdqi)NO](PF$_6$)$_3$ release from nitrosyl ruthenium-loaded SLN and NLC dispersed in different vehicles

In vitro release studies were performed using a Franz diffusion cell (Microette Apparatus, Hanson Research, Chatsworth, USA) at 37 °C. A cellulose acetate membrane (MWCO 12,000–14,000) was used as a support for the formulations. First, 300 μL of the SLN or NLC suspension at a concentration of 220 μg mL^{-1} was placed in the donor compartment (sink conditions considered), and the receiving compartment (7 mL) was filled with either Hepes Buffer (25 mmol L^{-1}, containing NaCl 133 mmol L^{-1} and at pH 7.4) or purified water. Samples from the receiving solution (600 μL) were collected from the Franz cells in the following intervals: 2, 4, 6, 8, 10, 12 and 18 h. The same volume of fresh receiving solutions was replaced. Samples were analyzed by the HPLC method as described above. Mathematical dilution adjustments were further considered to correctly determine the complex content in the samples.

Furthermore, in order to study the influence of the lyophilization process in the NRC release profile from the carriers, the experiments were also conducted with either SLN freshly prepared or lyophilized SLN resuspended in purified water.

2.6. Stability of [Ru(terpy)(bdqi)NO](PF$_6$)$_3$ in aqueous solution and in SLN as a function of time

The stability of NRC was assessed in solution and encapsulated in SLN for 30 days (n = 3) at 40 μg mL^{-1}. To perform these studies, freshly prepared [Ru(terpy)(bdqi)NO](PF$_6$)$_3$-loaded SLN suspensions and [Ru(terpy)(bdqi)NO](PF$_6$)$_3$ complex in aqueous solution were stored in hermetic glass flasks and protected from light at 4 °C (±2 °C), 25 °C (±2 °C) and 37 °C (±1 °C) (Laboratory oven, Fanem, Brasil). Additionally, the stability of lyophilized SLN loaded with

NRC, maintained in desiccator was also assessed. The flasks were collected and the samples were analyzed by HPLC after 1, 7, and 30 days. Prior to analysis, the samples were diluted employing a methanol:water solution (1:2); calibration curves were also prepared daily in methanol:water solution (1:2).

2.7. Stability of [Ru(terpy)(bdqi)NO](PF$_6$)$_3$ in contact with skin as a function of time

Suspensions of lyophilized SLN, just resuspended in purified water, or solutions, both at 10 μg mL^{-1} of NRC, were incubated with pig skin homogenates for 4 h. For this purpose, in a tube, 100 mg of skin was homogenized in purified water added with NRC dispersion for 1 min at 12,000 rpm (Ultra Turrax, AT15, IKA-Werke, Germany). The samples were then extracted to be further analyzed by HPLC after 0, 1, 2 and 4 h of skin contact. For the extraction procedure, 1 mL of methanol was added, and then the tube was centrifuged employing an LC-1 Excelsa Baby centrifuge (model II 206-R) at 1500 × *g* for 10 min. The supernatant was evaluated by HPLC in order to determine the remaining NRC after skin contact.

2.8. Photochemical studies

Photolysis of the complex was performed in solution (purified water), as has been reported for other nitrosyl ruthenium complexes [35]; the same procedure was performed for SLN suspensions. The reactor consisted of a 200-W light source and a high-pressure mercury lamp (Philips, Brazil) at wavelength 350–700 nm [35]. First, 20 mL of [Ru(terpy)(bdqi)NO](PF$_6$)$_3$ aqueous solution or [Ru(terpy)(bdqi)NO](PF$_6$)$_3$-loaded SLN at 40 μg mL^{-1} was irradiated while stirring in a glass flask for 180 min at 25 (±2) °C. Samples were withdrawn and submitted to HPLC analysis in order to determine the remaining [Ru(terpy)(bdqi)NO](PF$_6$)$_3$ after light exposition, indirectly indicating the amount of NO released.

In addition, NO release was also assessed using an amperometric NO sensor (NOmeter, ISO-NOP, World Precision Instruments, Sarasota, USA) coupled to a computer [15]. In this experiment, 2.5 mL of the NRC in solution or encapsulated in SLN (220 μg mL^{-1}) was trapped in a cellulose membrane bag immersed in purified water, then irradiated. The NO sensor immersed in the purified water was placed directly next to the cellulose bag and detected the NO that was released from the NRC and spread to the medium.

3. Results and discussion

3.1. Identification and validation of [Ru(terpy)(bdqi)NO](PF$_6$)$_3$ by HPLC

NRC determination in biological medium has already been validated [21], however, due to the differences between the biological samples, i.e. microsome [21] *versus* skin, the method was validated again to attain the new conditions. During the synthesis of the NRC, two isomers are formed [20]; the employed method was able to separate them. It was observed the elution of the first isomer at 10 min and the second one at 15.5 min, similarly as it has already been demonstrated by de Oliveira et al. [20,21]. The peak purities were further confirmed by employing an SPD-M10A VP diode array detector operating in the range of 200 to 550 nm (Shimadzu, Kyoto, Japan). Since there is no pharmacological information about each isomer, the results obtained here were expressed as the sum of the two isomers (peak 1 + peak 2) [21]. The method proved to be linear over the concentration range of 0.2–20 μg mL^{-1} ($y = 38342x - 9450.2$) for the NRC, with correlation coefficient (r) = 0.9998. The precision and accuracy of the method can be observed in Table 1. Neither RSDs nor relative errors exceeded a value of 6%. The lowest concentration quantified by the validated method (LOQs) was 0.2 μg mL^{-1} with RDS value and relative error below 9% and 10%, respectively. Blank lipid carriers, blank receiver solutions and blank skin homogenates showed no interferences in the retention times of the isomers. Recovery studies demonstrated recovery rates above 89.00%.

Table 1
Precision and accuracy for the analysis of [Ru(terpy)(bdqi)NO](PF$_6$)$_3$.

Nominal concentration (μg mL^{-1})	Obtained concentration (μg mL^{-1})	Accuracy (relative error, %)[a]	Precision (RSD, %)[b]
Within-day			
2.00	1.98	−0.82	2.79
5.00	5.02	0.02	2.66
10.00	10.60	4.25	3.90
Between-day			
2.00	2.02	4.75	4.09
5.00	5.08	0.11	2.92
10.00	10.52	5.28	2.20

[a] Expressed as deviation from theoretical values
[b] Expressed as relative standard deviation.

3.2. SLN and NLC preparation and characterization

[Ru(terpy)(bdqi)NO](PF$_6$)$_3$ is a potential anticancer compound that could be successfully employed in the treatment of malignances occurring in skin. Lipid nanoparticles, due to several previously described advantages, could be effectively employed for the delivery of such a drug. In this way, SLN were prepared. In addition, since it has been reported in literature that the nearly perfect crystalline structure formed in SLN leads to limited loading possibilities for drugs [26], NLC were also prepared by replacing a portion of stearic acid with oleic acid (liquid lipid), which could form a crystalline particle matrix with imperfections and thus increase the loading capacity. Studies were performed for the developed NRC-loaded lipid carriers in order to observe their particular characteristics and release profiles. The lipid carriers were characterized by photon correlation spectroscopy, zeta potential, scanning electron microscopy (SEM), and entrapment efficiency.

3.2.1. Photon correlation spectroscopy and zeta potential

SLN and NLC had average diameters in the nanometer scale range, with NLC showing a smaller average diameter than SLN (Table 2). The polydispersity index was close to 0.2 for all lipid carriers, suggesting a relatively narrow size distribution [27].

The analysis of zeta potential, which is the electric potential at the plane of shear, is a useful way to predict the physical storage stability of colloidal systems. Zeta potential values higher than |30 mV| show good stability during the shelf-life [27]. In the present study, [Ru(terpy)(bdqi)NO](PF$_6$)$_3$-loaded and -unloaded SLN and

Table 2
Average diameter, polidispersity index (PdI) and zeta potential obtained for [Ru(terpy)(bdqi)NO](PF$_6$)$_3$-loaded and unloaded SLN and NLC (n = 3).

Lipid carrier	Average diameter (nm)	Polidispersity index (PdI)	Zeta potential (mV)
Unloaded SLN	270 ± 38	0.25 ± 0.02	−38.7 ± 9.21
Loaded SLN	275 ± 15	0.24 ± 0.04	−40.7 ± 10.40
Unloaded NLC	227 ± 15	0.30 ± 0.04	−51.3 ± 9.46
Loaded NLC	211 ± 31	0.23 ± 0.07	−50.0 ± 7.50

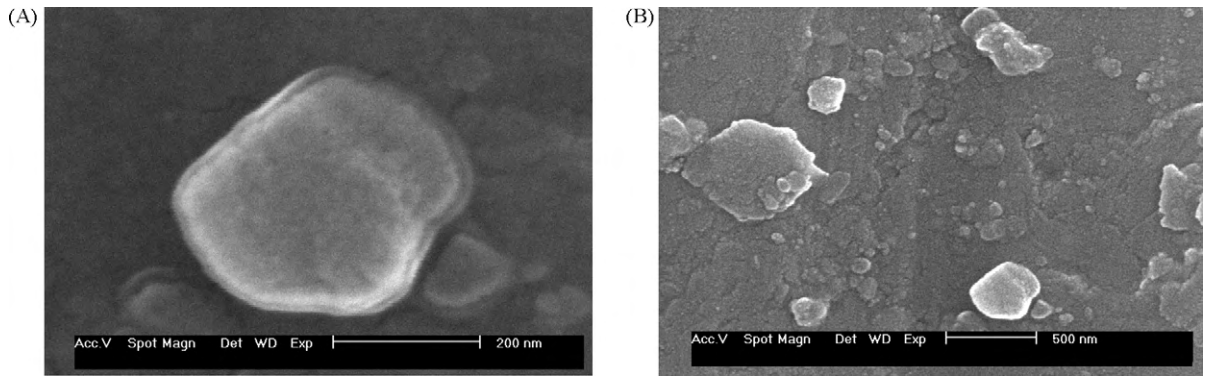

Fig. 2. Scanning electron microscopy (SEM) of SLN suspensions containing nitrosyl ruthenium complex.

NLC presented zeta potential between −38 and −51 mV. This range suggests that both suspensions might classify as physically stable since particle aggregation is not likely to occur under these conditions of electrostatic repulsion between the particles. Because oleic acid is negatively charged at its carboxylic groups, NLC revealed the highest zeta potential values, possibly due to the accumulation of oleic acid at the surface of the NLC [27].

3.2.2. Scanning electron microscopy (SEM)

Fig. 2 shows the image of [Ru(terpy)(bdqi)NO]$(PF_6)_3$-loaded SLN, which was similar to the other loaded and unloaded lipid carriers. As already demonstrated in the literature [27], the particles revealed an anisometric shape with a size of approximately 200 nm. A general agglomeration of particles can be observed due to the lipid nature of carriers and due to the sample preparation prior to SEM analysis. In the literature, spherical [36] and non-spherical shapes [37] of SLN and NLC have also been reported by transmission electron microscopy (TEM).

3.2.3. Entrapment efficiency

The NRC encapsulation efficiency was 78.32 ± 4.41% for SLN and 86.02 ± 1.59% for NLC. Therefore, the EE values observed demonstrate that the developed lipid carriers had high entrapment efficiency. It has been reported that high entrapment efficiency may be related to the incorporation of the drug in the surfactant layer at the surface of the lipid carrier [38]. During the microemulsion formation the drug can partition from the oil phase to the aqueous phase, however, during the cooling of the O/W microemulsion, the solubility of the drug in the water phase can decrease, leading to the re-partition of the drug to the lipid phase. When the lipid recrystallization temperature is reached, a solid lipid core starts forming that includes the drug, which is present at this temperature in this lipid phase. The already-crystallized core is no longer accessible for the drug; consequently the drug concentrates in the still liquid outer shell of the SLN and/or on the surface of the particles [39]. Based on this discussion and on knowing the physicochemical characteristics of the NRC, such as water solubility at room temperature (718.02 $\mu g\,mL^{-1}$) and octanol/water partition coefficient ($\log K_{O/W} = -1.70$, determined using the shake-flask method), it might be supported that the developed lipid carriers could follow the core-shell model (drug enriched shell) [39] in drug incorporation and corroborates the results observed in the release profiles of NRC from the lipid carriers (reported below).

3.3. In vitro kinetics of [Ru(terpy)(bdqi)NO]$(PF_6)_3$ release from nitrosyl ruthenium-loaded SLN and NLC dispersed in different vehicles

In vitro release kinetic studies were conducted in order to select a suitable vehicle for dispersing the lipid carriers. Since the SLN and NLC are the drug delivery systems for the NRC topical administration, it would be necessary that the complex remain in the lipid carrier while the delivery system is on the skin. Once the NRC-loaded lipid carrier penetrates the skin, the complex should be released so it can subsequently release the NO ligand into the skin. Therefore, NO release control can be provided not only by light irradiation, but also by the kinetics of release of the NRC from the SLN.

Studies have reported release experiments performed with SLN dispersed in buffer solution [40], in gel formulations [41], and in purified water [31]. Therefore, the [Ru(terpy)(bdqi)NO]$(PF_6)_3$ release from the lipid carriers were evaluated first in Hepes buffer medium, then in purified water medium. Additionally, the influence of SLN lyophilization in NRC release from the lipid carriers was assessed.

The [Ru(terpy)(bdqi)NO]$(PF_6)_3$ release profiles in Hepes buffer medium are presented in Fig. 3A. It can be observed that 60.5 ± 7.36% of the NRC in solution diffuses through the cellulose acetate membrane (dialysis membrane) over 2 h, reaching 72.0 ± 11.4% after 4 h. Although the solution and the lipid carrier release rates bear some superficial similarities, the differences between them are remarkable. The NRC release rates from SLN and NLC were about 60.5% in 4 h, reaching 70% after 8 h of experiment. The statistical analysis showed that SLN and NLC presented significantly lower [Ru(terpy)(bdqi)NO]$(PF_6)_3$ release rates ($p < 0.05$) throughout a 4 h experiment compared to the solution.

Based on these results, it is possible to conclude that the lipid carriers sustained moderate loss of [Ru(terpy)(bdqi)NO]$(PF_6)_3$. Also noteworthy is the fact that the presence of oleic acid in the NLC did not result in any difference in the release of ruthenium complex from the SLN.

In order to explore the influence of ionic force on the NRC release from SLN, purified water was also employed as the receptor medium (Fig. 3B). In this condition, the drug release rate from the lipid carrier only reached 60.5 ± 7.6% after 18 h of experiment. Clearly, the ionic force had a strong effect on the NRC release performance. Significantly lower amounts of NRC were observed compared to the study performed in isotonic Hepes medium over both 4 h and 12 h experiments. In light of this, it can be suggested that when the NLC and the NRC incorporated in the surfactant layer at the surface of the SLN are exposed to electrolyte-containing media, a typical ion exchange mechanism leads to a higher drug release from the particle. This feature should be examined when choosing the vehicle for administration of these carriers to the skin surface.

The results obtained in this study are in agreement with Wong et al. [31], who stated that the presences of ion in the receptor medium did promote increased release rate of anticancer drugs from lipid carriers. Similar results have been observed by Ruckmani et al. [32] using methotrexate (MTX)-loaded SLN.

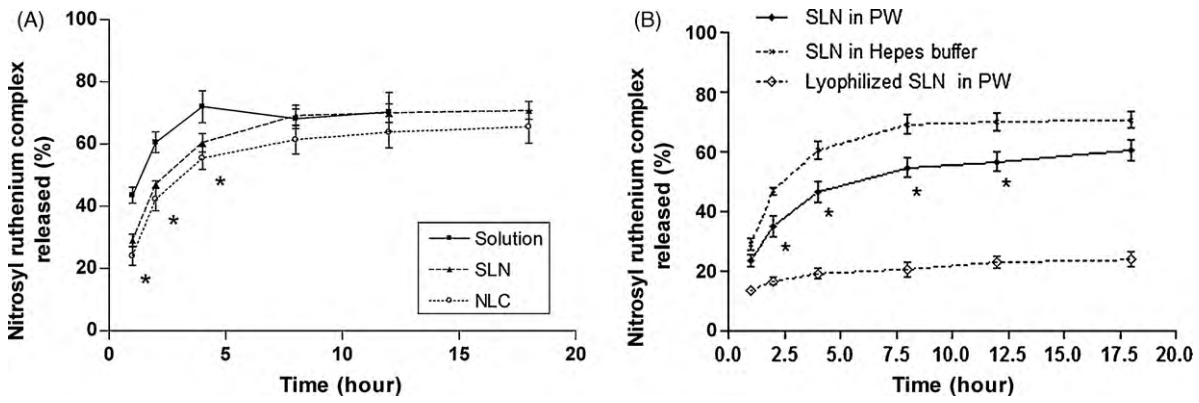

Fig. 3. Percentage of [Ru(terpy)(bdqi)NO](PF$_6$)$_3$ released as a function of time. (A) Experiment performed in medium consisting of Hepes buffer (25 mmol L^{-1}, with NaCl 133 mmol L^{-1}, pH 7.4); (B) Experiment performed in medium consisting of purified water. Data are means ± SEM of experiments ($n \geq 6$) performed in different days. *$p \leq 0.05$, representing statistically lower release rate from the control (A: both SLN and NLC were compared to the solution; B: SLN in buffer medium was compared to SLN in purified water) employing *t*-test followed by Mann–Whitney test.

Despite performing the *in vitro* release experiments in sink conditions (but with a finite dose), the plateau attained for NRC formulations, with maximum release rates of around 80%, remains (Fig. 3A). It is noteworthy to emphasize that mathematical dilution adjustments were performed after each sample withdrawn. It is possible that a small amount of the complex had been entrapped into the dialysis membrane used as the formulation support. Also of importance is the consideration of the uncontrolled NO release from NRC, once the NO release generates other ruthenium complexes that are not quantified here. In this context, the stability of the NRC in aqueous solution and in the SLN was studied as described below (Section 3.4).

Besides evaluating the vehicle influence, the SLN lyophilization was also explored regarding to the NRC release rate. In Fig. 3B, it can be observed that over the 18-h experiment, the NRC release from the lyophilized SLN reached around 22% (significantly lower [Ru(terpy)(bdqi)NO](PF$_6$)$_3$ release rates ($p < 0.05$, *t*-test) compared to non-lyophilized SLN) meaning that the lyophilization process is probably changing the SLN inner structure and sustaining the NRC release.

3.4. Stability of [Ru(terpy)(bdqi)NO](PF$_6$)$_3$ in aqueous solution and in SLN as a function of time

The stability of the NO ligand association with the ruthenium complex was evaluated by HPLC. The NO release from the complex generates other complexes, such as the aqua complex ([Ru(terpy)(bdqi)H$_2$O](PF$_6$)$_3$) [15], which presents another retention time in the chromatographic analysis. Therefore, the decrease in the NRC detected by the HPLC analysis would indicate the NO release from the complex. As this NRC is a new compound, no studies have been reported in literature regarding its stability in either aqueous solution or in a pharmaceutical formulation, such as SLN. Thus this study is of notable importance, since this complex is a prominent therapeutic agent and contaminants present in the medium may influence its stability.

Fig. 4A and B shows the remaining percentage of ruthenium complex in aqueous solution and in SLN suspension as a function of time and temperature. It can be observed that the temperature did affect the stability of [Ru(terpy)(bdqi)NO](PF$_6$)$_3$. After 7 days of storage at 37 °C, the remaining ruthenium complex was about 40%, both in solution and SLN suspensions. After 30 days of storage at these conditions, the samples could not be evaluated since they were lower than the method quantification limit (0.2 μg mL^{-1}). Regarding to the NRC in solution, it was observed that the storage at 4 °C lead to the complete stability of the complex for 30 days. However, this was not accomplished by the NRC-loaded SLN in suspension. The results suggest that the SLN in suspension did not improve NRC stability in the conditions evaluated, probably due to reducing agents present in the solution medium and in the SLN suspension. The reducing influence of the lipids in SLN is confirmed in the photochemical studies described in Section 3.6.

In view of this, the plateaus reached in the release study (with release rates lower (80%) than the expected ones (100%)) might be partly due to the degradation of the drug (Fig. 3A). In fact, in the 24 h study at 37 °C, a decrease in the NRC content of about 20% was observed both in solution and in SLN, with no statistical difference between the formulations ($p > 0.05$). However, when the release rates of NRC from the solution and the lipid carriers were compared in the *in vitro* release study, the lower amount of NRC found in the

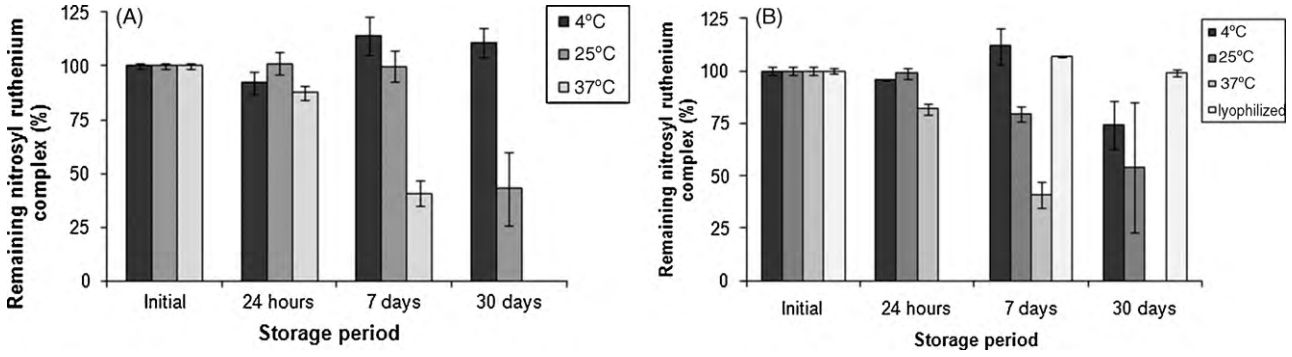

Fig. 4. Remaining percentage of [Ru(terpy)(bdqi)NO](PF$_6$)$_3$ in solution (A) and in SLN suspension and lyophilized SLN (B). The samples were stored at 4 °C (±2 °C), 25 °C (±2 °C) and 37 °C (±1 °C) ($n = 3$). The lyophilized SLN was maintained in dissecator at room temperature.

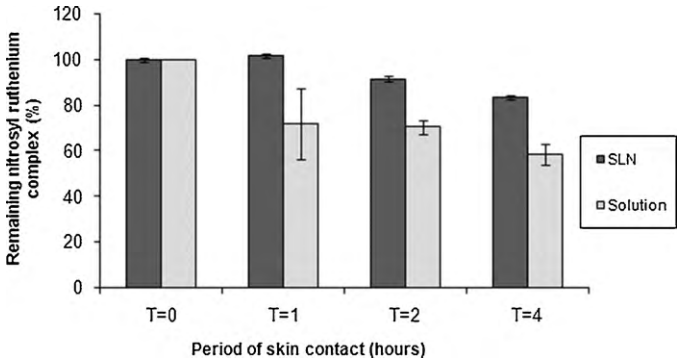

Fig. 5. NRC stability in contact with skin in function of time. Comparison between the remaining NRC in solution and loaded in SLN after 0, 1, 2 and 4 h of skin homogenate contact.

receiving compartment from the SLN (Fig. 3A) was closely related to the slow release rate of the drug from the lipid carrier, not to the degradation of the complex.

While this increase in NO release due to the SLN carrier is interesting for the therapeutic effect of the NO, it cannot be released prior to the application of the formulation on the skin. To overcome this subject, NRC-loaded SLN was lyophilized and its storage in desiccator permitted the complete stability of the NO ligand for at least 30 days as demonstrated in Fig. 4B.

3.5. Stability of [Ru(terpy)(bdqi)NO](PF$_6$)$_3$ in contact with skin as a function of time

Once the NRC has presented instabilities in reducing environments and it is expected that the NRC-loaded SLN will be further applied against skin disorders, skin homogenates were used to evaluate the influence of encapsulation in the NRC stability. It was observed that the remaining concentration of NRC in contact with skin was time dependent and the encapsulation in SLN influenced this stability. Fig. 5 shows that after 1, 2 and 4 h of skin contact, the remaining NRC was 71.75 ± 15.72%, 70.47 ± 3.01% and 58.27 ± 4.44% when in solution and 101.71 ± 8.60%, 91.54 ± 5.92 and 83.36 ± 4.71% when encapsulated in SLN, respectively (Fig. 5). Therefore, the encapsulation improved the NRC stability in a significant way ($p < 0.05$, t-test).

It is believed that the reducing environment found, which is obviously overestimated from the real situation found in normal skin due to the experimental conditions (homogenization of the skin), is leading to the NO release from the NRC and, the encapsulation is protecting the NRC reduction. As it was exposed in Section 3.2, the NRC release rate from lyophilized SLN in water after 4 h is 19.22%. This percentage is very close to the NRC degradation determined in this period (16.64%), indicating that once released from the particle, the NRC is no more protected, and the NO is released.

Therefore, after released from the particle, the NRC reduction triggered by skin contact leads the NO release, which depending on the concentration can lead to cell death. Generally speaking, Thomas et al. [42] stated that relative low concentrations of NO (≤300 nM) tend to favor progrowth and antiapoptotic responses, whereas higher levels of NO (~1 μM) favor pathways that induce cell-cycle arrest, senescence, or apoptosis. In this regard, due to the capacity of SLN in controlling NRC release and protecting it from early reduction, this system could be employed to modulate the concentrations of NO in cancerous tissues localized in skin. Additionally, it is well known that the NRC reduction can also be controlled by light irradiation, as forwarded described, and this approach could be combined with the NRC modulation by SLN to reach biological effects.

3.6. Photochemical studies

It has been reported that light irradiation leads to NO release from the [Ru(terpy)(bdqi)NO](PF$_6$)$_3$ complex; the NO then forms its aqua photo-products as can be observed in Schemes 1 and 2 [15]. Therefore, the solutions and SLN suspensions were irradiated under glass flasks where most of the light irradiation is in the wavelength ≥350 nm, enabling the evaluation of $[Ru^{III}(terpy)(bdqi)H_2O]^{3+}$ formation and other products originating from secondary photochemical pathways.

The photolysis of NRC was performed in solution (purified water) and in a SLN water suspension in order to observe the influence of formulation compounds on the NO release from the complex. The evaluations were carried out in two sets of experiments.

In the first set, indirect photorelease of NO from NRC in solution or loaded in SLN was determined by HPLC (Fig. 6A). In this study, the remaining NRC content was quantified after irradiation. A gradual decrease in NRC content was observed as function of irradiation time, as shown in Fig. 6B. The HPLC analysis revealed two NRC isomers; to obtain more information about this issue, see reference [20].

In solution, it was determined that after 90 and 180 min of light irradiation, the NRC released around 7.73 ± 1.64% and 18.21 ± 2.65% of NO, respectively. In contrast, when encapsulated in SLN, the NRC had already released around 16.35 ± 7.15% of NO in the first 90 min of irradiation, and 32.91 ± 8.13% of NO after 180 min. It may be suggested that the compounds present in SLN are influencing the reduction of the nitrosyl ligand and improving the NO release by about 2-fold in the presence of light (350–700 nm). One possible mechanism involved in nitrosyl ruthenium reduction may be the formation of superoxide anions ($O_2^{\bullet -}$), which are formed during the oxidation of fat acids in the presence of O_2 under light irradiation [43].

To elucidate that the decrease in NRC content after light irradiation determined by HPLC-indicated NO release, a second set of experiments were performed using a NO sensor. Immediately after exposing the solution and SLN to irradiation (Fig. 7) the chronoamperogram displayed current increases detected by the specific electrode, indicating the photochemical production of NO. Fig. 7 shows a higher current with the irradiation of NRC-loaded

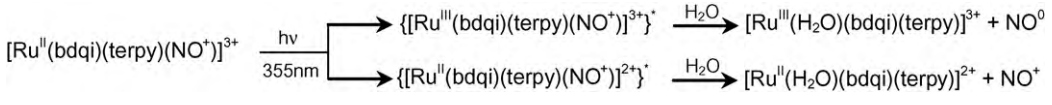

Scheme 1. Aqua photo-products obtained after [Ru(terpy)(bdqi)NO](PF$_6$)$_3$ is subjected to light irradiation at 355 nm [15].

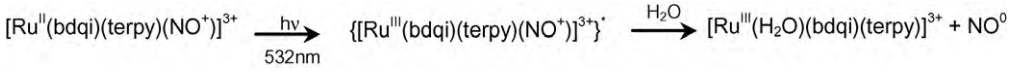

Scheme 2. Aqua photo-product obtained after [Ru(terpy)(bdqi)NO](PF$_6$)$_3$ is subjected to light irradiation at 532 nm [15].

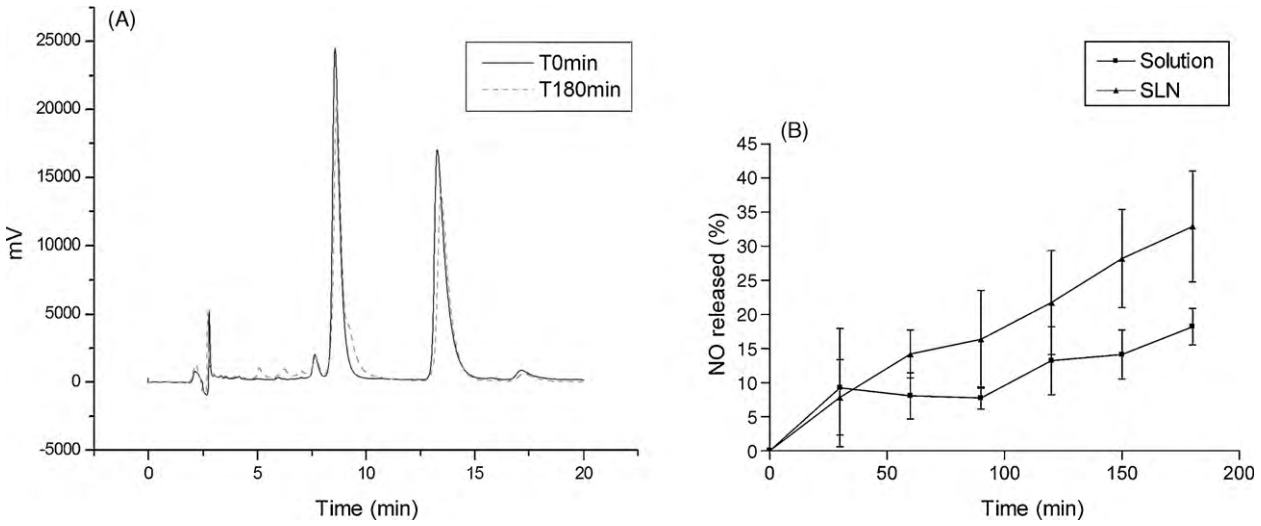

Fig. 6. (A) Chromatograms referring to the separation of [Ru(terpy)(bdqi)NO]$(PF_6)_3$ isomers during irradiation. Solid line = 0 min; dash line = 180 min of irradiation; (B) NO released (in percentage) as a function of time from [Ru(terpy)(bdqi)NO]$(PF_6)_3$ in solution and in SLN suspension.

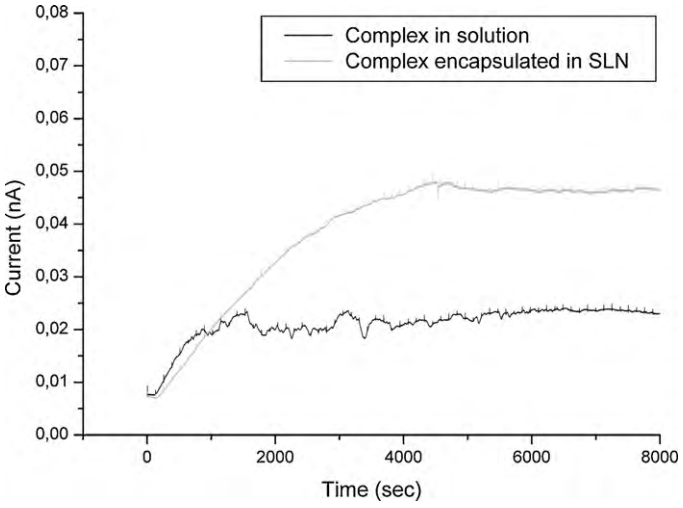

Fig. 7. Chronoamperogram. Time course of NO release from the [Ru(terpy)(bdqi)NO]$(PF_6)_3$ complex under visible light irradiation in function of time assayed by NO meter.

SLN compared to NRC in solution, corroborating the results found in the HPLC analysis.

The photochemical studies confirmed that the UV–vis light irradiation really triggered the NO release from NRC and this approach may be useful to improve the NRC reduction, especially from SLN. Because a specific portion of UV spectrum, the UVA-1 (340–400 nm) region, can penetrate deeper into skin [44], the light irradiation could be employed after some period of SLN skin permeation in order to permit a burst of NO release from NRC, improving the NO concentration into the skin. Investigations of the SLN skin penetration *in vitro* and *in vivo* are currently in progress in our laboratory.

4. Conclusions

The [Ru(terpy)(bdqi)NO]$(PF_6)_3$-loaded SLN and NLC presented suitable average diameter, zeta potential, entrapment efficiency, and release kinetics to be compatible with topical application. The ionic strength of the vehicle was observed to promote NO release from the complex; therefore, the lipid carriers should be lyophilized and dispersed in an ion free-vehicle just before administration, avoiding premature NO release. Besides controlling the NRC release kinetics, the SLN also improved considerably the stability of this drug in contact with skin homogenates. Additionally, the photochemical studies showed that [Ru(terpy)(bdqi)NO]$(PF_6)_3$-loaded SLN increased the NO release after light irradiation.

Acknowledgements

This work was supported by grants from Coordenação de Aperfeiçoamento de Pessoal de Nível Superior (CAPES), Conselho Nacional de Desenvolvimento Científico e Tecnológico (CNPq), and Fundação de Amparo à Pesquisa do Estado de São Paulo (FAPESP).

References

[1] L.J. Ignarro, Nitric Oxide: Biology and Pathobiology, first ed., Academic Press, San Diego, 2000.
[2] M.J. Rose, P.K. Mascharak, Photoactive ruthenium nitrosyls: effects of light and potential application as NO donors, Coord. Chem. Rev. 252 (2008) 2093–2114.
[3] G.R.J. Thatcher, An introduction to NO-related therapeutic agents, Curr. Top. Med. Chem. 5 (2005) 597–601.
[4] A.R. Butler, I.L. Megson, Non-heme iron nitrosyls in biology, Chem. Rev. 102 (2002) 1155–1166.
[5] S. Mocellin, V. Bronte, D. Nitti, Nitric oxide, a double edged sword in cancer biology: searching for therapeutic opportunities, Med. Res. Rev. 27 (2007) 317–352.
[6] A.M. Simeone, S. Colleta, R. Krahe, M.M. Jhnson, E. Mora, A.M. Tari, N-(4-Hydroxyphenyl)retinamide and nitric oxide pro-drugs exhibit apoptotic and anti-invasive effects against bone metastatic breast cancer cells, Carcinogenisis 27 (2006) 568–577.
[7] K. Karidi, A. Garoufis, A. Tsipis, N. Hadjililadis, H. den Dulk, J. Reedijk, Synthesis, characterization, in vitro antitumor activity DNA-binding properties and electronic structure (DFT) of the new complex cis-(Cl,Cl)[$Ru^{II}Cl_2(NO^+)$(terpy)]Cl, Dalton Trans. 7 (2005) 1176–1187.
[8] L.G.F. Lopes, E.E. Catellano, A.G. Ferreira, C.U. Davanzo, M.J. Clarke, D.W. Franco, Reactivity of *trans*-[$Ru(NH_3)_4P(OEt)_3NO]X_3$ ($X = PF_6^-$, CF_3COO^-): modulation of the release of NO by the *trans*-effect, Inorg. Chim. Acta 358 (2005) 2883–2890.
[9] D. Bonaventura, F.S. Oliveira, V. Togniolo, A.C. Tedesco, R.S. da Silva, L.M. Bendhack, A macrocyclic nitrosyl ruthenium complex is a NO donor that induces rat aorta relaxation, Nitric Oxide 10 (2004) 83–91.
[10] V. Togniolo, R.S. da Silva, A.C. Tedesco, Photo-induced nitric oxide release from chlorobis(2,2′-bipyridine)nitrosylruthenium(II) in aqueous solution, Inorg. Chim. Acta 316 (2001) 7–12.
[11] F.D. Oliveira, V. Togniolo, T.T. Pupo, A.C. Tedesco, R.S. da Silva, Nitrosyl ruthenium complex as nitric oxide delivery agent: synthesis, characterization and photochemical properties, Inorg. Chem. Commun. 7 (2004) 160–164.
[12] M.G. Sauaia, F.S. Oliveira, A.C. Tedesco, R.S. da Silva, Control of NO release by light irradiation from nitrosyl–ruthenium complexes containing polypyridyl ligands, Inorg. Chim. Acta 355 (2003) 191–196.
[13] M.G. Sauaia, R.G. de Lima, A.C. Tedesco, R.S. da Silva, Photoinduced NO release by visible light irradiation from pyrazine-bridged nitrosyl ruthenium complexes, J. Am. Chem. Soc. 125 (2003) 14718–14719.

[14] M.G. Sauaia, F.S. Oliveira, R.G. de Lima, A.D.L. Cacciari, E. Tfouni, R.S. da Silva, Syntheses, characterization and photochemical properties of new NO•–ruthenium(II) complexes, Inorg. Chem. Commun. 8 (2005) 347–349.
[15] R.G. de Lima, M.G. Sauaia, D. Bonaventura, A.C. Tedesco, R.F.V. Bendhack, R.S. da Silva, Influence of ancillary ligand L in the nitric oxide photorelease by the $[Ru(L)(tpy)NO]^{3+}$ complex and its vasodilator activity based on visible light irradiation, Inorg. Chim. Acta 359 (2006) 2543–2549.
[16] R.G. de Lima, M.G. Sauaia, C. Feresin, I.M. Pepe, N.M. José, L.M. Bendhack, Z.N. da Rocha, R.S. da Silva, Photochemical and pharmacological aspects of nitric oxide release from some nitrosyl ruthenium complexes entrapped in sol–gel and silicone matrices, Polyhedron 26 (2007) 4620–4624.
[17] D. Bonaventura, R.G. De Lima, J.A. Vercesi, R.S. da Silva, L.M. Bendhack, Comparison of the mechanisms underlying the relaxation induced by two nitric oxide donors: sodium nitroprusside and a new ruthenium complex, Vasc. Pharmacol. 46 (2007) 215–222.
[18] R.G. de Lima, M.G. Sauaia, D. Bonaventura, A.C. Tedesco, R.F.V. Lopez, L.M. Bendhack, R.S. da Silva, Controlled nitric oxide photo-release from nitro ruthenium complexes: the vasodilator response produced by UV light irradiation, Inorg. Chim. Acta 358 (2005) 2643–2650.
[19] G. Von Poefhsitz, A.L. Bogado, M.P. de Araujo, H.S. Selistre-de-Araujo, J. Ellena, E.E. Castellano, A.A. Batista, Synthesis, characterization X-ray structure and preliminary in vitro antitumor activity of the nitrosyl complex fac-$[RuCl_3(NO)(dppf)]$, dppf = 1,1′-bis(diphenylphosphine)ferrocene, Polyhedron 26 (2007) 4707–4712.
[20] A.R.M. de Oliveira, F. Marquele-Oliveira, D.C.A.S. de Santana, S. Nikolaou, P.S. Bonato, R.S. da Silva, HPLC separation, NMR and QTOF/MS/MS structure elucidation of a prominent nitric oxide donor agent based on an isomeric composition of a nitrosyl ruthenium complex, Inorg. Chem. Commun. 12 (2009) 343–346.
[21] A.R.M. de Oliveira, P. da Fonseca, C. Curti, R.S. da Silva, P.S. Bonato, *In vitro* metabolism study of a new nitrosyl ruthenium complex $[Ru(NH{\cdot}NHq)(terpy)NO]^{3+}$ nitric oxide donor using rat microsomes, Nitric Oxide 21 (2009) 14–19.
[22] P. Vallance, J. Collier, Fortnightly review biology and clinical relevance of nitric oxide, Br. Med. J. 309 (1994) 453–457.
[23] M. Schäfer-Korting, W. Mehnert, H.C. Korting, Lipid nanoparticles for improved topical application of drugs for skin diseases, Adv. Drug Deliv. Rev. 59 (2000) 427–443.
[24] S.F. Taviera, A. Nomizo, R.F.V. Lopez, Effect of the iontophoresis of a chitosan gel on doxorubicin skin penetration and cytotoxicity, J. Control. Release 134 (2009) 35–40.
[25] R.H. Müller, M. Radtke, S.A. Wissing, Solid lipid nanoparticles (SLN) and nanostructured lipid carriers (NLC) in cosmetic and dermal dermatological preparations, Adv. Drug Deliv. Rev. 54 (Suppl. 1) (2002) S131–S155.
[26] R.H. Müller, Lipid nanoparticles: recent advances, Adv. Drug Deliv. Rev. 59 (2007) 375–376.
[27] V. Teeranachaideekul, E.B. Souto, V.B. Junyaprasert, R.H. Müller, Cetyl palmitate-based NLC for topical delivery of coenzyme Q_{10}: development, physicochemical characterization and in vitro release studies, Eur. J. Pharm. Biopharm. 67 (2007) 141–148.
[28] K.A. Shah, A.A. Date, M.D. Joshi, V.B. Patravale, Solid lipid nanoparticles (SLN) of tretinoin: potential in topical delivery, Int. J. Pharm. 345 (2007) 163–171.
[29] R. Sivaramakrishnan, C. Nakamura, W. Mehnert, H.C. Korting, K.D. Kramer, M. Schäfer-Korting, Glucocorticoid entrapment into lipid carriers – characterisation by parelectric spectroscopy and influence on dermal uptake, J. Control. Release 97 (2004) 493–502.
[30] C.S. Maia, W. Mehnert, M. Schäfer-Korting, Solid lipid nanoparticles as drug carriers for topical glucocorticoids, Int. J. Pharm. 196 (2000) 165–167.
[31] H.L. Wong, R. Bendayan, A.M. Rauth, X.Y. Wu, Development of solid lipid nanoparticles containing ionically complexed chemotherapeutic drugs and chemosensitizers, J. Pharm. Sci. 93 (2004) 1993–2008.
[32] K. Ruckmani, M. Sivakumar, P.A. Gebeshkumar, Methotrexate loaded solid lipid nanoparticles (SLN) for effective treatment of carcinoma, J. Nanosci. Nanotechnol. 6 (2006) 2991–2995.
[33] FDA, Guidance for Industry Bioanalytical Method Validation, Center for Drug Evaluation and Research, 2001, http://www.fda.gov/cder/guidance/4252fnl.fdf.
[34] A.S. Pattani, S.D. Manawgade, V.B. Patravale, Development and comparative anti-microbial evaluation of lipid nanoparticles and nanoemulsion of polymyxin B, J. Nanosci. Nanotechnol. 6 (2006) 1–5.
[35] F.S. Oliveira, T.M.B. Ramos, S.S.M. Oliveira, R.S. da Silva, C.M. de Gaitani, J.M. Marchetti, Development of biodegradable nanoparticles containing trans-$[RuCl([15]ane)^{2+}$ as nitric oxide donor, Trends Inorg. Chem. 10 (2008) 27–34.
[36] E. Ugazio, R. Cavalli, M.R. Gasco, Incorporation of cyclosporine A in solid lipid nanoparticles (SLN), Int. J. Pharm. 241 (2002) 341–344.
[37] A. Saupe, S. Wissing, A. Lenk, C. Schmidt, R.H. Müller, Solid lipid nanoparticles (SLN) and nanoestructured lipid carriers (NLC) – structural investigations on two different carriers systems, Biomed. Mater. Eng. 15 (2005) 393–402.
[38] W. Tiyaboonchai, W. Tungpradit, P. Plianbangchang, Formulation and characterrization of curcuminoids loaded solid lipid nanaoparticles, Int. J. Pharm. 337 (2007) 299–306.
[39] R.H. Müller, K. Mäder, S. Gohla, Solid lipid nanoparticles (SLN) for controlled drug delivery – a review of the state of the art, Eur. J. Pharm. Biopharm. 50 (2000) 161–177.
[40] H. Yuan, L.L. Wang, Y.Z. Du, J. You, F.Q. Hu, S. Zeng, Preparation and characteristics of nanostructured lipid carriers for control-releasing progesterone by melt-emulsification, Colloids Surf. B 60 (2007) 174–179.
[41] M. Joshi, V. Patravale, Nanostructured lipid carrier (NLC) based gel of celecoxib, Int. J. Pharm. 346 (2008) 124–132.
[42] D.D. Thomas, L.A. Ridnou, J.S. Isenberg, W. Flores-Santana, C.H. Switzer, S. Donzelli, P. Hussain, C. Vecoli, N. Paolocci, S. Ambs, C.A. Colton, C.C. Harris, D.D. Roberts, D.A. Wink, The chemical biology of nitric oxide: implications in cellular signaling, Free Radic. Biol. Med. 45 (2008) 18–31.
[43] B. Halliwell, J.M.C. Gutteridge, Free Radicals in Biology and Medicine, third ed., Pergamon Press, New York, 1999.
[44] M. Weichenthal, T.T. Schwarz, Phototherapy: how does UV work? Photodermatol. Photoimmunol. Photomed. 21 (2005) 260–266.